



# Radiation exposure dose outside the irradiation field due to differences in pediatric head computed tomography scanning methods

Kenta Higuchi<sup>1</sup> · Takuya Fujimura<sup>2</sup>

Received: 9 August 2020 / Revised: 8 March 2021 / Accepted: 10 March 2021 / Published online: 30 March 2021  
© Japanese Society of Radiological Technology and Japan Society of Medical Physics 2021

## Abstract

The use of pediatric computed tomography (CT), a valuable imaging tool, has been increasing rapidly. The present study examined radiation exposure in non-irradiated fields of CT scans in pediatric patients using a 7-year-old child phantom. Radio-photoluminescence glass dosimeters were placed in the insertion ports of the phantom corresponding to the organs. For the helical and the non-helical scans, the doses to the head in the irradiation field were 54.6 mGy and 53.4 mGy, respectively. The dose measured for the helical scan was 2.3% higher than that for the non-helical scan. The largest dose was in the thyroid gland, and the doses for helical and non-helical scans were 5.37 mGy and 3.58 mGy, respectively. The difference in the dose between helical and non-helical scans was 1.79 mGy. The dose measured for the helical scan was 50% higher than that for the non-helical scan. The dose to which the thyroid gland was exposed outside the irradiation field in the head CT scan was 5.37 mGy using the helical scan method. The excess relative risk per gray increased by 3–5.5% if the excess relative risk per gray was 5–10. Decreasing the dose to the thyroid gland, which has a high risk of cancer after radiation exposure, is desirable. The dose to the thyroid gland was higher in the helical scan than in the non-helical scan. This is probably because overscanning, which is unique to helical scanning, increases the exposure dose outside the irradiation field.

**Keywords** Radiation exposure · Non-target fields · Computed tomography · Children · Pediatrics

## 1 Introduction

The use of pediatric computed tomography (CT), a valuable imaging tool, has rapidly increased [1]. According to the Organization for Economic Co-operation and Development Health Statistics 2020 [2], Japan has 101.3 CT scanners per million population, which is the highest globally. The ionizing radiation doses delivered by a CT scan are 100–500 times higher than those delivered by the conventional radiography [3]. Pediatric CT scans are a public health concern due to the following reasons:

1. Children are known to be more sensitive to radiation than adults.
2. Children have a longer life expectancy than adults, resulting in a larger window of opportunity for expressing radiation damage.
3. Children may receive a higher radiation dose than necessary if CT settings are not adjusted for their smaller body size [4–9].

Several studies have found an increased risk of cancer associated with CT scans among children. A recent study in the United Kingdom reported that the risk of leukemia in children who underwent CT and received a red bone marrow dose of  $\geq 30$  mGy was 3.2 times greater and the risk of brain cancer in those who underwent CT and received a brain dose of  $\geq 50$  mGy was 2.8 times greater than in those who received a dose of  $< 5$  mGy [10]. An Australian study conducted by John Mathews and his team from the University of Melbourne examined the Medicare and cancer records of almost 11 million subjects aged up to 19 years. In

✉ Kenta Higuchi  
rt.khiguchi@gmail.com

<sup>1</sup> Department of Radiological Sciences, Faculty of Health Sciences, Japan Health Care College, Shinei, Kiyota-ku, Sapporo 434-104-0839, Japan

<sup>2</sup> Department of Medical Radiological Technology, Kagoshima Medical Technology College, 5417-1, Hirakawa, Kagoshima 891-0133, Japan

this study, children who had undergone CT had a 24% higher chance of developing cancer than those who had not [11].

As discussed above, several epidemiological studies have shown that pediatric CT may increase the risk of cancer in organs irradiated during CT examinations. However, information on non-irradiated organs is limited. The CT-scan radiation dose was administered to a 7-year-old child phantom rather than a patient. According to a previous study, various types of medical examinations were performed in infants and children (0–15 years) in well-developed countries; the percentages of head, chest, abdominal, and spine CT examinations performed in children were 8%, 5%, 4%, and 3%, respectively [4]. The most frequent CT examinations are for the head, accounting for 40% of all pediatric CT scans. In this study, the dose of radiation exposure to irradiation and non-irradiation fields from CT scans was examined.

## 2 Materials and methods

### 2.1 Imaging device

The CT-scan device used in this study was a 16-slice multi-detector CT scanner (Brivo CT 385, General Electric Healthcare, Chicago, IL, USA). Scanning was conducted three times for the helical and non-helical data acquisition methods. These two scanning methods were used, because their radiation doses in non-irradiated fields may differ [12]. The scan range was from the foramen magnum to the parietalis capitis region, thus, covering the entire brain. Auto exposure control (AEC) was not used to prevent variations in the imaging conditions due to the AEC and perform the CT scan under similar conditions using the same phantom.

Brivo CT 385 does not have a gantry tilt function. Therefore, the gantry was not tilted in any imaging procedure. After performing a head CT scan, Brivo CT 385 reconverts the image data into an image using the orbitomeatal line (OM line) as the reference plane. This is a smart position function (digital tilt) that automatically constructs an image. The Brivo CT 385 uses a digital tilt to acquire tilted images without tilting the gantry. This is achieved by reconstructing the 0° image using the background algorithm.

### 2.2 Imaging conditions

This study measured radiation exposure of irradiation (head) and non-irradiation fields of CT scans using a 7-year-old child phantom (THRA2, Kyoto Kagaku Co., Ltd.) mainly consisting of epoxy resin. This human torso phantom is made of soft tissue (WE-211), lung tissue (LP-430), and bone tissue (BE-303) equivalent materials and cut at 25–30 mm [13–17]. Diagnostic reference levels (DRLs) were incorporated into the international guidelines of the International

Commission on Radiological Protection (ICRP) and the International Atomic Energy Agency (IAEA). DRLs are the standard for medical radiological protection in the diagnostic field. Therefore, in this study, we referred to the DRLs. Scanning conditions were set up, such that CT dose index volumes (CTDI<sub>vol</sub>s) and dose length products (DLPs) were similar to those indicated by the DRLs of the Japan Network for Research and Information on Medical Exposures (J-RIME) for pediatric patients aged 6–10 years [18]. The scanning conditions used in this study are listed in Table 1. We irradiated 60 mGy, which is the 75% value described in Japan DRLs 2015. The 75% value listed in Japan DRLs 2020 has changed to 55 mGy, with a median of 39 mGy. Therefore, in this study, the irradiation was 1.5 times more than the median.

The quality of CT images can be quantified by the standard deviation (SD) of 2.3–2.6 in ROI. The ideal SD value differs from organ to organ. In general, this value must be between and 3–5 [19]. In this study, three ROIs were selected, and their average values were calculated. The obtained SD values were in the range of 2.3–2.6, indicating the good quality of the obtained images (Table 1). The coefficients of variation (CV) were in the range of 0.1%–0.79%. The average and 95% confidence intervals (95% CIs) of CVs were 0.217% and 0.193–0.241, respectively. The doses for the non-helical and helical scanning ranges were similar in both age groups. For the helical and non-helical

**Table 1** Scanning conditions for helical and non-helical scans

| Scanning methods          | Scanning conditions for those aged 6–10 years |             |
|---------------------------|---|-------------|
|                           | Helical                                       | Non-helical |
| X-ray tube voltage        | 120 kV  | 120 kV      |
| X-ray tube current        | 140 mA  | 150 mA      |
| Rotating time             | 2.0 s   | 2.0 s       |
| Slice thickness           | 5 mm  | 5 mm        |
| Beam width                | 5 mm  | 5 mm        |
| Image number taken        | 26  | 26          |
| Helical pitch             | 0.938: 1                                      | –           |
| Overlapped area           | 0.31 mm                                       | –           |
| CTDI <sub>vol</sub> *     | 60.6 mGy                                      | 60.9 mGy    |
| DLP**                     | 1020.8 mGy                                    | 791.3 mGy   |
| SD of the CT level in ROI | 2.6   | 2.3         |

CTDI<sub>vol</sub> computed tomography dose index volumes

\*CTDI<sub>vol</sub> displayed on the operator console in a computed tomography system

DLP dose length product

\*\*DLP displayed on the operator console in a computed tomography system

SD standard deviation

ROI region of interest

scan methods, the scan area was 16.8 cm and 13.0 cm, respectively.

### 2.3 Measurements of radiation doses

The thyroid gland, thymus, breast, and ovary/testis were selected as measurement organs based on the ICRP report [1]. Radio-photoluminescence glass dosimeters (RPLDs) of AGC Techno Glass Company were placed in the insertion ports and the surface of the phantom, corresponding to thyroid gland, thymus, breast, and ovary/testis.

The glass element used was GD-302 M as it was suitable for the size of the dosimeter inserted into the hole inside the pediatric human phantom used in this study. However,

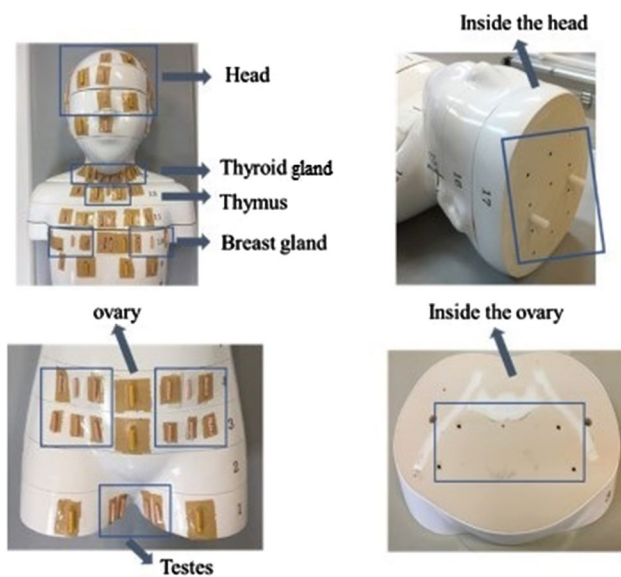


**Fig. 1** RPLD positions. As measurement organs, the thyroid, thymus, breast, and ovary/testis were selected on the basis of the report of International Commission on Radiological Protection (ICRP). Radio photoluminescence glass dosimeters (RPLDs) of AGC Techno Glass Company were placed in the insertion ports of the phantom, corresponding to these organs

because the relative response differs according to the type of glass element, corrections were performed using a calibration constant. The calibration constant was calculated as follows: the GD-302 M and GD-352 M were installed in a pediatric phantom, and CT imaging was performed in and out of the irradiation field under the same scanning conditions. The correction factor was calculated from the ratio of the absorbed doses of GD-302 M and GD-352 M. CT imaging was performed three times using 20 glass dosimeters. The glass dosimeters repeated the reading ten times to confirm that the readings did not fluctuate. Before reading the value, the irradiated glass element was subjected to a predetermined heat treatment in a preheated incubator to stabilize the fluorescent component of the glass element. The positions of the RPLDs are shown in Fig. 1. Because the external ear canal is the reference point for CT imaging, we set it to zero. Glass dosimeters were placed as follows: 17 in the brain, 5 in the thyroid gland, 1 in the thymus, 4 in the breast, 8 in the ovary, and 4 in the testis. Doses were measured thrice, and the mean doses were calculated. The dose measured by the RPLD was considered as the absorbed dose (mGy).

## 3 Results

### 3.1 Doses measured with RPLDs

As expected, organ doses measured using RPLD and a 7-year-old child phantom decreased with increasing distance from the irradiation zone (Table 2). The relationship between the distance from the external ear canal and the dose of each organ is shown for helical and non-helical scans (Fig. 2). The average dose for each organ was estimated based on the measured dose. For the helical and the non-helical scans, the dose to the head in the irradiation field was 54.6 mGy and 53.4 mGy, respectively. The difference between them was 1.25 mGy. The dose measured for the helical scan was 2.3% higher than that for the non-helical scan.

**Table 2** Organ doses measured using RPLD and a 7-year-old child phantom

| Organ   | Distance (cm) from external ear canal to each organ | Measured doses (mGy) |                 |                  |  |
|---------|---|----------------------|-----------------|------------------|--|
|         |   | Scanning methods     |                 | Difference : a-b | Percentage of difference (%) : (a-b)/b*100 |
|         |   | Helical (a)          | Non-helical (b) |                  |  |
| Brain   | 0.0   | 54.6                 | 53.4            | 1.25             | 2.34                                       |
| Thyroid | 6.0   | 5.37                 | 3.58            | 1.79             | 50.0                                       |
| Thymus  | 9.0   | 2.95                 | 1.89            | 1.06             | 56.1                                       |
| Breast  | 15.0  | 1.64                 | 1.12            | 0.52             | 46.4                                       |
| Ovary   | 33.0  | 0.13                 | 0.11            | 0.02             | 18.2                                       |
| Testis  | 42.0  | 0.09                 | 0.08            | 0.01             | 12.5                                       |

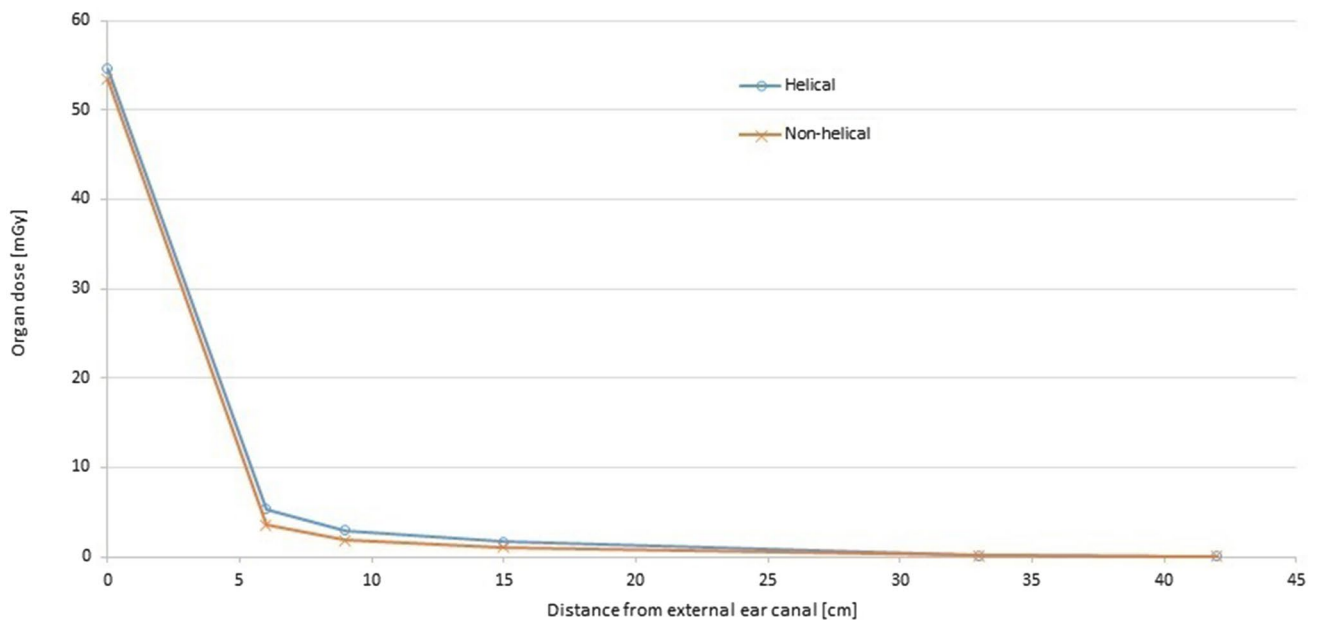


**Fig. 2** The relationship between the organ dose and the distance. The relationship between the distance from the external ear canal and the dose of each organ was shown for helical and non-helical scans

The largest dose was in the thyroid gland, and the doses using helical and non-helical scans were 5.37 mGy and 3.58 mGy, respectively. The difference in the dose between helical and non-helical scans was 1.79 mGy. The dose measured for the helical scan was 50.0% higher than that for the non-helical scan.

For helical and non-helical scans, doses in the thymus were 2.95 mGy and 1.89 mGy, respectively. The differences were 1.06 mGy. The dose measured for the helical scan was 56.1% higher than that for the non-helical scan.

For helical and non-helical scans, doses in the breast were 1.64 mGy and 1.12 mGy, respectively; the difference was 0.52 mGy. The dose measured for the helical scan was 46.4% higher than that for the non-helical scan.

For helical and non-helical scans, doses in the ovary were 0.13 mGy and 0.11 mGy, respectively; the difference was 0.02 mGy. The dose measured for the helical scan was 18.2% higher than that for the non-helical scan.

For helical and the non-helical scans, doses in the testis were 0.09 mGy and 0.08 mGy, respectively; the difference was 0.01 mGy. The dose measured for the helical scan was 12.5% larger than that for the non-helical scan.

## 4 Discussion

### 4.1 Differences between helical and non-helical scans

An important difference between helical and non-helical scans is overscanning, in which the scan range is wider than planned. Overscanning is caused by the presence of pitch during helical scanning.

In this study, the pitch was 0.938:1. Because the pitch was shorter than one, at a scan, its bed-moving distance was shorter than the beam width. As a result, the same part (0.31 mm) was irradiated twice, affecting the dose measured with the RPLDs. It occurs not only at the beginning of scanning but also its end [20].

In the case of non-helical scanning, the bed-moving distance was the same as the scan range. Although not shown in the results, the difference between helical and non-helical scanning ranges was 3.84 cm.

In head CT, the crystalline lens may be exposed. In particular, the helical scan method has the risk of increasing the exposure dose owing to the influence of overscanning.

**Table 3** Difference between doses measured with RPLD and reported doses

| Scanning method | Measured doses (a) | Displayed doses * (b) | Difference (mGy) : a-b | Percentage of difference (%) : (a-b)/a*100 |
|-----------------|--------------------|-----------------------|------------------------|--|
| Helical         | 54.6               | 60.6                  | -6.0                   | -11  |
| Non-helical     | 53.4               | 60.9                  | -7.5                   | -14  |

\*Displayed dose: dose value displayed on the operator console in a computed tomography system

## 4.2 Differences between measured dose and dose value displayed on the operator console

The radiation dose used in a CT scan is generally displayed on a CT device. However, there is a possibility that the actual radiation dose received differs from that displayed on the CT device. Therefore, it was compared with the radiation dose measured by the RPLDs.

The reported dose calculation assumes the use of an acrylic head phantom, which is a cylinder with a diameter of 16 cm. Its differences from our THRA2 phantom of Kyoto Kagaku in materials and structures were important contributors to the observed differences.

For the helical and the non-helical scans, differences between measured and reported doses were 6.00 and 7.47 mGy, respectively (Table 3). The doses measured with RPLDs were 11–14% smaller than those reported by the device.

The tendency for the estimated value to be high can increase the awareness of the radiation exposure of the imaging technologist. However, there is a probability of overestimation of the risk of CT scans.

## 4.3 Cancer risk

For the helical scan, the thyroid gland absorbed doses in non-irradiated fields were approximately one-tenth of the irradiation head absorbed doses. The measured doses estimated the average dose to the thyroid gland as 5.37 mGy.

In a pooled analysis of children aged < 15 years, Ron et al. reported that the excess relative risk (ERR) per Gy was 5–10 [21, 22]. The risks when irradiating with 60 mGy, which is the 75% value described in Japan DRLs 2015, are as follows. On CT examinations of the head, the largest dose was in the thyroid gland, and the dose was 5.37 mGy. CT examination of the head in children may increase the risk of thyroid cancer in children by 3–5.4%.

The calculation formula is shown as follows:

$$5 \text{ ERR/Gy} \times 5.37 \times 10^{-3} \text{ Gy} \times 100\% = 3\%$$

$$10 \text{ ERR/Gy} \times 5.37 \times 10^{-3} \text{ Gy} \times 100\% = 5.4\%$$

In addition, the risk when irradiating with a median value of 39 mGy described in Japan DRLs 2020 are 2%–3.4%.

The calculation formula is shown as follows:

$$5 \text{ ERR/Gy} \times 5.37 \times 10^{-3} \text{ Gy} \times 100\% \times (39 \text{ mGy}/60 \text{ mGy}) = 2\%$$

$$10 \text{ ERR/Gy} \times 5.37 \times 10^{-3} \text{ Gy} \times 100\% \times (39 \text{ mGy}/60 \text{ mGy}) = 3.4\%$$

However, this should not be overlooked. Although many medical personnel are aware of the exposure dose in the irradiation field, the level of awareness of doses outside the irradiation field and the magnitude of its risk is low. Doses outside the irradiation field to the thyroid gland from pediatric head CT scans may increase the risk of thyroid cancer and cannot be overlooked.

The exposure dose outside in the irradiation field was higher in helical scanning than in non-helical scanning. This is probably because overscanning, unique to helical scanning, increases the exposure dose outside the irradiation field. Usually, in a helical scan accompanied by movement of the bed, there is an X-ray irradiated area at the start and end of the scan that does not contribute to the image reconstruction. Radiation that is unnecessary for image diagnosis can be reduced by cutting this area with a collimator. However, it can only reduce the dose delivered up to 20% [23, 24].

## 5 Conclusion

Decreasing the dose to the thyroid gland, which has a high risk of cancer after radiation exposure, is desirable. The dose to the thyroid gland was higher in the helical scan than in the non-helical scan. This is due to the overscanning that is unique to helical scan technology.

**Acknowledgements** The authors thank Prof. S. Akiba, Prof. T Yoshimura, Prof. C Koriyama, and Dr. M Toyota for their invaluable contributions to this project.

**Funding** None.

## Declarations

**Conflict of interest** The authors declare that they have no conflict of interest.



## References

- International Commission on Radiological Protection (ICRP). Managing Patient Dose in Computed Tomography. ICRP Publication 87. Ann. 2000; ICRP 30 (4).
- Organisation for Economic Co-operation and Development (OECD). OECD Health Statistics 2020. OECD. Stat, Health Care Resources: Medical technology, <https://stats.oecd.org/Index.aspx?QueryId=30184>, (accessed 2020–11–20).
- United Nations Scientific Committee on the Effects of Atomic Radiation (UNSCEAR). Sources and effects of ionizing radiation. Report to the General Assembly of the United Nations with Scientific Annexes, Annex D: Medical radiation exposures, United Nations sales publication. 2000: New York.
- United Nations Scientific Committee on the Effects of Atomic Radiation (UNSCEAR). Sources and effects of ionizing radiation. UNSCEAR 2013 Report. Volume II. Scientific Annex B: Effects of radiation exposure of children. United Nations sales publication E.14.IX.2. United Nations, New York 2013.
- Committee to Assess Health Risks from Exposure to Low Levels of Ionizing Radiation and National Research Council. Health Risks from Exposure to Low Levels of Ionizing Radiation: BEIR VII Phase 2. 2006: The National Academies Press; Washington, D.C.
- Chodick G, Ronckers CM, Shalev V, Ron E. Excess lifetime cancer mortality risk attributable to radiation exposure from computed tomography examinations in children. *Isr Med Assoc J*. 2007;8:584–7.
- Miglioretti DL, Johnson E, Williams A, Greenlee RT, Weinmann S, Solberg LI, et al. Pediatric computed tomography and associated radiation exposure and estimated cancer risk. *JAMA Pediatr*. 2013;167:700–7.
- Gao Y, Quinn B, Mahmood U, Long D, Erdi Y, Germain J, et al. A comparison of pediatric and adult CT organ dose estimation methods. *BMC Med Imaging*. 2017;17:28.
- Gao Y, Quinn B, Pandit-Taskar N, Behr G, Mahmood U, Long D, et al. Patient-specific organ and effective dose estimates in pediatric oncology computed tomography. *Phys Med*. 2018;45:146–55.
- Pearce MS, Salotti JA, Little MP, McHugh K, Lee C, Kim KP, et al. Radiation exposure from CT scans in childhood and subsequent risk of leukaemia and brain tumours: a retrospective cohort study. *Lancet*. 2012;380:499–505.
- Mathews JD, Forsythe AV, Brady Z, Butler MW, Goergen SK, Byrnes GB, et al. Cancer risk in 680 000 people exposed to compute tomography scans in childhood or adolescence: data linkage study of 11 million Australians. *BMJ*. 2013;346:F2360.
- Miyazaki O, Horiuchi T. Pediatric CT Practice. *Journal of Japanese Society of Pediatric Radiology*. 2006;22:33–43.
- ICRU report 44: Tissue Substitutes in Radiation Dosimetry and Measurement, ICRU, Bethesda, Maryland, 1989.
- Hiraoka T. Basic data for phantom materials, (1) Radiation therapy phantom. *Medical Standard DOSE*. 1999;4(1):23–8 ((in Japanese)).
- Hiraoka T. Basic data for phantom materials, (2) Mass attenuation coefficients, Vol.4 No.2, 17–23, 1999. (in Japanese)
- Hiraoka T. Basic data for phantom materials, (3) Mass absorption coefficients, Vol.4 No.2, 25–31, 1999. (in Japanese)
- Hiraoka T. Basic data for phantom materials, (4) Stopping power and Limited stopping power, Vol.5 No.1, 33–63, 2000. (in Japanese)
- Japan Network for Research and Information on Medical Exposures (J-RIME). National diagnostic reference levels in Japan (2020). Japan DRLs 2020. [http://www.radher.jp/J-RIME/report/JapanDRL2020\\_jp.pdf](http://www.radher.jp/J-RIME/report/JapanDRL2020_jp.pdf)
- Kodera S. Photographing technique of head CT. From basic to clinical. *RT*. 2007;38:71–76. (in Japanese).
- Banno T. Usefulness for the radiation exposure reduction of synchronization asymmetry Z-axis collimation at the time of the helical scan. *Tohoku Journal of Radiological Technology*. 2012;21:112–3 ((in Japanese)).
- Preston DL, Ron E, Tokuoka S, Funamoto S, Nishi N, Soda M, et al. Solid Cancer Incidence in Atomic Bomb Survivors: 1958–1998. *Radiat Res*. 2007;168:1–64.
- Ron E, Lubin JH, Shore RE, Mabuchi K, Modan B, Pottern LM, Schneider AB, Tucker MA, Boice JD Jr. Thyroid cancer after exposure to external radiation: a pooled analysis of seven studies. *Radiat Res*. 1995;141:259–77.
- Tzedakis A, Damilakis J, Perisinakis K, Stratakis J, Gourtsoyannis N. The effect of z overscanning on patient effective dose from multidetector helical computed tomography examinations. *Med Phys*. 2005;32:1621–9.
- Tzedakis A, Damilakis J, Perisinakis K, Karantanas A, Karabekios S, Gourtsoyannis N. Influence of z overscanning on normalized effective doses calculated for pediatric patients undergoing multi-detector CT examinations. *Med Phys*. 2007;34:1163–75.

**Publisher's Note** Springer Nature remains neutral with regard to jurisdictional claims in published maps and institutional affiliations.